J. exp. Biol. 140, 1-33 (1988)
Printed in Great Britain © The Company of Biologists Limited 1988

MUSCULAR MECHANISMS OF SNAKE LOCOMOTION: AN ELECTROMYOGRAPHIC STUDY OF THE SIDEWINDING AND CONCERTINA MODES OF *CROTALUS CERASTES, NERODIA FASCIATA* AND *ELAPHE OBSOLETA*

BY BRUCE C. JAYNE
Developmental and Cell Biology, University of California, Irvine, CA 92717, USA

Accepted 11 May 1988

Summary

Synchronized electromyography and cinematography were used to determine the muscle activity of colubroid snakes during sidewinding and concertina locomotion. The primary muscles studied were the three largest, most superficial epaxial muscles: the Mm. semispinalis-spinalis, longissimus dorsi and iliocostalis. Sidewinding locomotion of *Nerodia fasciata* and *Crotalus cerastes* was the result of continuous posterior propagation of contractile blocks consisting of several adjacent muscle segments. During sidewinding, the activity of the M. longissimus dorsi and M. iliocostalis was primarily unilateral, beginning when a body region was convex and ending when it was maximally concave on the side of the active muscle. Unilateral activity of the M. semispinalis-spinalis correlated with lateral flexion in addition to bilateral activity that correlated with dorsiflexion of the vertebral column. During concertina locomotion of *N. fasciata* and *Elaphe obsoleta*, muscle activity also involved blocks of several simultaneously active adjacent muscle segments, but all major activity was unilateral and was not propagated posteriorly in a simple continuous fashion. Muscle activity during concertina locomotion correlated either with lateral flexion towards the side of the active muscle or with the maintenance of static contact with the sides of a tunnel. The number of simultaneously active adjacent muscle segments and the maximum duration of continuous muscle activity varied significantly between *Nerodia* and *Elaphe* and among the different widths of tunnels. Theoretical considerations combined with observed differences suggest that the more elongate body of *Elaphe* is advantageous for performing concertina locomotion. There was no consistent evidence that nonhomologous muscles with tendinous interconnections functioned as single units during either of these two locomotor modes. Although individual segments of the studied epaxial muscles span several vertebrae, *via* long, tendinous connections, consistent kinematic correlations with muscle activity were observed only between the contractile portion of a muscle segment and the vertebrae adjacent to that contractile portion.

Introduction

Previous work on lower vertebrate locomotion has emphasized the great

Key words: locomotion, snakes, muscle, electromyography.

importance of axial movement (Gray, 1968; Gans, 1974). However, with the exception of recent work (Jayne, 1988) no previous study has experimentally measured axial muscle activity during the terrestrial locomotion of any reptile. Within the many lineages of lower vertebrates that have independently evolved limblessness, snakes are by far the most diverse (Gans, 1974; Edwards, 1985). Despite the parallel study of snake axial musculature (Mosauer, 1935; Gasc, 1967, 1974; Jayne, 1982) and kinematics of locomotion (Mosauer, 1932; Gray & Lissmann, 1950; Gans, 1974; Jayne, 1986), little is known about muscle activity during snake locomotion. Jayne (1988) used electromyography to test the models of Gray & Lissmann (1950) and Gray (1953) and found that snakes performing terrestrial lateral undulation move by the continuous posterior propagation of alternating unilateral muscle activity. However, the muscle activity used during two other major terrestrial locomotor modes of sidewinding and concertina are completely unknown.

Three generalizations have emerged from anatomical studies of snake axial musculature (Mosauer, 1935; Gasc, 1967, 1974; Jayne, 1982). First, there is a major dichotomy in the arrangement of muscles of primitive (booid) *versus* advanced (colubroid) snakes. Second, within the colubroid snakes, there are different patterns of tendinous interconnections between non-homologous muscles such as the semispinalis and the longissimus dorsi. Third, the percentage of the total number of body vertebrae spanned by axial muscle segments and the relative proportion of tendon to contractile tissue within a muscle varies markedly within colubroid snakes, and this variation is correlated with specializations for locomotion and constriction.

One important finding of previous kinematic studies of snake locomotion is that most snakes change locomotor mode in response to the resistive forces generated by the substrate (Gray & Lissmann, 1950). In the absence of anteromedially directed irregularities that are sufficient for lateral undulation, snakes often perform either sidewinding or concertina locomotion (Gans, 1974). Within the confines of parallel-sided tunnels burrowing snakes rely heavily on the concertina mode. Hence, an investigator can study different locomotor modes without using different taxa because of this response of snakes to experimental manipulation of the substrate.

In this study I used synchronized electromyography and cinematography to determine the muscular mechanisms of the sidewinding and concertina modes. I primarily determined the activity of the three largest epaxial muscles, the Mm. semispinalis-spinalis, longissimus dorsi and iliocostalis. Only colubroid snakes were used to minimize the variation in the morphology of these muscles. The primary species studied were the colubrids *Nerodia fasciata pictiventis* (Cope) (Florida banded watersnake) and *Elaphe obsoleta quadrivittata* (Holbrook) (yellow rat snake) and the viperid *Crotalus cerastes* (Hallowell) (sidewinder rattlesnake). Of these species, *N. fasciata* is behaviourally and morphologically the most generalized, with an axial anatomy characteristic of non-constricting snakes (Jayne, 1982). *E. obsoleta* has a combination of segmental muscle lengths and large numbers of vertebrae that is a characteristic specialization of constricting colubroids, and *C. cerastes* appears to be morphologically and behaviourally specialized for sidewinding (Jayne, 1982; Gans & Mendelssohn, 1972).

This study had the following five specific goals. First, muscle activity was described for: (1) sidewinding of the generalized *Nerodia fasciata* and the specialized *Crotalus cerastes* and (2) concertina locomotion in tunnels of *N. fasciata* and the specialized *Elaphe obsoleta*. Second, the muscle activity characteristic of each locomotor mode was determined by comparing the shared features observed for the generalized–specialized species pairs. Third, tunnel width was varied to test its effect on muscle activity during concertina locomotion and to determine if it differentially affected *Nerodia* and *Elaphe* which have different numbers of body vertebrae and differ in stoutness. Fourth, regimes of vertebral flexion are compared among locomotor modes and are related to stoutness. Fifth, the activity of interconnected muscles was compared across all locomotor modes and species to test whether interconnected axial muscle segments have obligate synchronous activity.

Materials and methods

Specimens of *Nerodia fasciata* and *Elaphe obsoleta* were obtained from commercial suppliers in southern Florida and *Cerastes cerastes* were from a dealer in southern California. When possible, large individuals of each species were preferentially chosen so that the size of the epaxial muscles was maximized. For sidewinding, two *N. fasciata* and six *C. cerastes* were used. For concertina locomotion, five *N. fasciata* and four *E. obsoleta* were studied. Table 1 summarizes the lengths and masses of snakes used in this study and specifically mentioned in this text. A complete listing of snakes used can be found in Jayne (1985*b*).

Substrates were chosen which best elicited a particular locomotor mode (see Jayne, 1986). Sidewinding snakes crawled on either sand or a linoleum floor. For

Table 1. *Anatomical data for snakes cited in the text*

Snake	Mode	Sex	Mass (g)	Length (cm) Total	Length (cm) SV	Vertebrae Total	Vertebrae Body
NF36	SW	M	76	68	48	212	126
NF33	C	F	280	91	71	176	125
NF40	C	F	330	100	78	197	127
EO15	C	F	510	126	118	265	240
EO21	C	M	490	159	130	327	237
CC5	SW	F	140	57	53	160	145
CC6	SW	M	155	58	53	165	146

Nerodia fasciata, Elaphe obsoleta and *Crotalus cerastes* are abbreviated NF, EO and CC, respectively.

Sidewinding and concertina are abbreviated SW and C, respectively. SV = snout–vent length.

concertina locomotion, wooden boards lined with dense rubber matting formed the parallel sides of tunnels which had a glass top and bottom. In addition to the individual snakes that were tested with a constant tunnel width, for each of two *Elaphe* and one *Nerodia*, trials were performed with tunnel widths of 5·0, 7·5 and 10·0 cm. Snakes were filmed moving at ambient room temperature (24–28 °C).

After filming, snakes were killed with an injection of sodium pentabarbitol. Snout–vent (SV) and tail lengths were then measured to the nearest centimetre and mass was determined to the nearest gram. Snakes were then fixed in 10 % formalin and stored in 70 % ethanol.

The electrodes used for electromyography were made of 0·051 mm diameter, poly-coated, stainless-steel wire. A cyanoacrylate glue was used to bond together about the first 10 cm of the strands of each bipolar electrode. With the aid of a dissecting microscope, a razor blade was used to scrape the insulation from the first 0·8–1·2 mm of the electrode wire. The bipolar electrodes were inserted through the skin and into muscles using 26 gauge hypodermic needles. A unipolar ground wire was implanted lateral to the ribs. After insertion, the electrode wires were glued to the skin of the snake using a cyanoacrylate glue with a viscous formula (advertised for bonding leather and wood). Small pieces of plastic were pressed against the glue to facilitate strong bonding. Plastic cement was then used to glue together the two strands of each electrode and to bond the electrodes to each other to form a single cable which was glued to the back of the snake. The lengths of electrode wire from the snake to the probes of the polygraph ranged from 1·5 to 3·0 m, averaging about 2 m. Lengths of wire were used that allowed unimpeded locomotion by the snakes. The number of bipolar electrodes (sets) implanted in a single snake ranged from four to 10.

Electromyograms (EMGs) were only used from electrodes whose positions were later confirmed by dissection of the preserved specimens. Preliminary experiments and dissection revealed that different times of EMG onset and offset were detectable from electrodes in different segments of homologous muscles that were as close as three vertebrae apart.

The EMGs were processed by a Grass model 7D polygraph with wide-band EEG alternating-current amplifiers (models 7P5B and 7P3B). EMGs were not integrated. High-pass and low-pass filter settings were 10 Hz and 40 kHz, respectively. A 60 Hz filter was also used to minimize noise. Depending on the availability of equipment, EMGs were recorded from 4–6 muscles simultaneously. The sensitivities of the preamplifiers varied from 50–300 μV cm^{-1}. The amplified signals were recorded on magnetic tape at 38·1 cm s^{-1} with a Honeywell model 5600 eight-channel tape recorder.

EMGs were played back from the tape recorder at 2·4 or 4·8 cm s^{-1} to the pens of the polygraph to provide a paper copy of the signals. Select sequences of EMGs, including those shown in the figures, were filtered with a 100 Hz high band pass filter before being played through a Gould model 220 pen recorder. These EMG records were analysed primarily for the onset and offset of muscle activity (to nearest 0·01 s). If the amplitude of the EMG varied greatly for a single muscle, intervals with a maximum amplitude of less than one-third the overall maximum were designated as low-level activity.

A Bolex H16 ciné camera operated at 50 frames s^{-1} with an exposure time of 1/300 s was used to obtain 16 mm films of snakes. The camera was always positioned vertically above the surfaces upon which the snakes crawled. Within view of the camera, a light blinked every 0·5 s simultaneously sending a signal to the tape recorder to synchronize the film and EMG records.

Films were projected using a Lafayette stop action projector. At regular time intervals, tracings were made of paint marks along the mid-dorsal scales of the snakes (Fig 1; see Jayne, 1988, for more detailed methods). These tracings provided a record of displacement that was digitized using a graphics tablet interfaced to an Apple II+ microcomputer. Linear velocities of points on the snake relative to the substrate and angular displacements within the vertebral column of the snake were calculated from the digitized records. Fig. 1A shows the method of calculating mean lateral vertebral flexion ($\bar{\theta}$) for intervals of four vertebral joints. Positive values of $\bar{\theta}$ indicate that the vertebral column is concave (flexed) to the animal's right. Fig. 1B shows that tracings were oriented so that the overall direction of travel was in the positive x direction and movement to the right was in the positive y direction (Jayne, 1986). Hence each overall linear velocity (V_r) could be resolved into forward (V_x) and lateral (V_y) components (Fig. 1B).

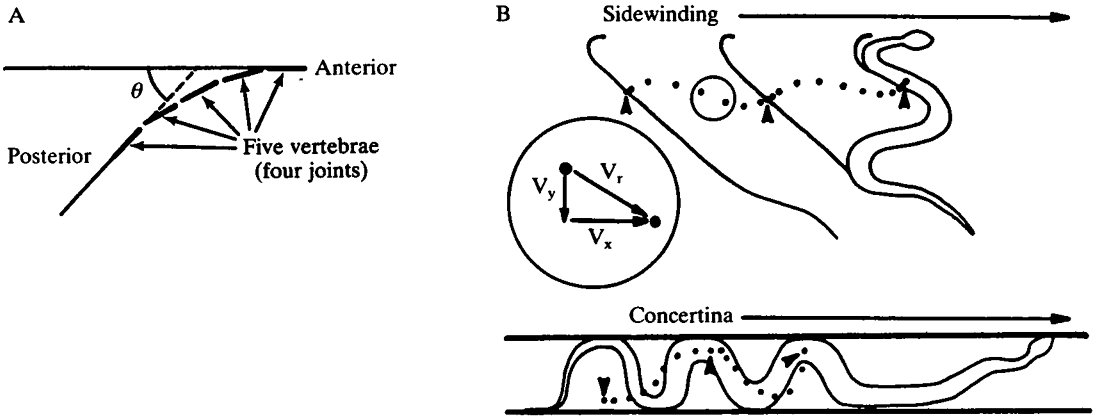

Fig. 1. Methods of measuring kinematic variables. (A) Method of measuring average vertebral flexion ($\bar{\theta}$). Angles were determined from line segments drawn through tracings of every fifth vertebra, and $\bar{\theta} = \theta/4$ where positive and negative values indicate concave (flexed) right (illustrated) and left, respectively. (B) Orientation of axes for determining linear velocities from a single point on a snake. The long horizontal arrows indicate the overall direction of travel for each snake. The dots indicate the record of displacement for a point on the snake measured using equal time intervals, and arrowheads indicate overlapping dots representing times of static contact. The inset shows the calculation of forward (V_x, positive = forward) and lateral (V_y, positive = right) components of the overall velocity (V_r). An example of right-handed sidewinding is shown, and the oblique lines behind this snake represent the impressions left by a snake moving on sand.

After converting all linear velocities to total snake lengths per second ($\mathrm{TL\,s^{-1}}$), plots of V_x, V_y and V_r *versus* time were used to determine locomotor mode (Jayne, 1986). Muscle activity was superimposed on plots of $\bar{\theta}$, V_y and V_r *versus* time to determine the mechanical correlates of EMGs. Unless otherwise stated, representative kinematic profiles are shown only for vertebral intervals that were adjacent to the belly of the muscle segment containing the electrode of interest.

Analysis of variance (ANOVA) was performed using the PC+ version of SPSS. Tukey's procedure was used to determine which group means differed significantly.

Results

Anatomy

The following descriptions of muscles are based on the average of measurements taken from at least three individuals each of *Crotalus cerastes*, *Nerodia f. pictiventris*, and *Elaphe o. quadrivittata*. Terminology follows that of Gasc (1981). Rather than describing all the axial muscles, descriptions are only provided for those muscles into which electrodes were implanted. For more complete accounts of the axial musculature, the reader is referred to Mosauer (1935) and Gasc (1974, 1981). Illustrations of the axial muscles of *N. fasciata* and *E. obsoleta* can be found in Jayne (1985*a*) and Jayne (1988), respectively.

In snakes, the three largest and most superficial longitudinal columns of epaxial muscles consist of segments of the Mm. semispinalis-spinalis (SSP-SP), longissimus dorsi (LD) and iliocostalis (IC). In all three colubroid species, the muscular segments of these three muscles each receive the majority of muscle fibres from two adjacent vertebral units (e.g. see spinalis origin on vertebrae 14 and 15 in Fig. 2). Despite this, certain tendinous portions of all three muscles exhibit a 1:1 correspondence with the vertebrae. These tendinous portions are (1) the long anterior tendon (AT) of the SSP-SP, (2) the anterior tendinous arch (TA) of the

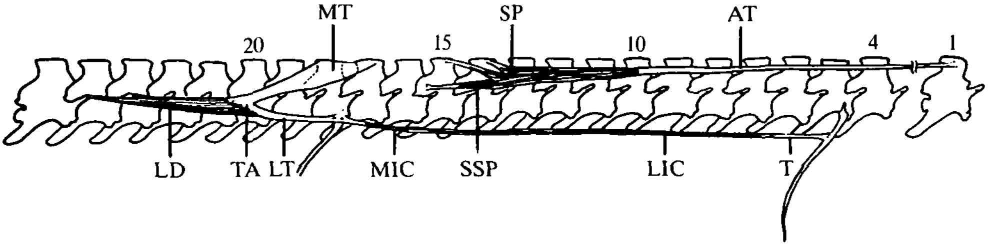

Fig. 2. Simplified right lateral view of the major epaxial muscle segments of *Crotalus cerastes*. Anterior is to the right. SP and SSP, respectively, indicate the spinalis and semispinalis portions of the M. semispinalis-spinalis, and AT is the anterior tendon of the SSP-SP. LD represents the M. longissimus dorsi and MT, TA and LT are the medial tendon, tendinous arch and lateral tendon of LD, respectively. MIC and LIC, respectively, are the medial and lateral heads of the M. iliocostalis and T is the anterior tendon of the LIC. See text for more detailed description. Vertebrae are numbered.

M. longissimus dorsi, and (3) the tendon (T) arising from the anterior portion of the lateral head of the M. iliocostalis (Fig. 2).

To facilitate comparisons, the vertebra onto which the anterior tendon of the SSP-SP inserted was counted as number one and the subsequent numbering of vertebrae proceeded posteriorly. Fig. 2 illustrates a simplified view of the arrangements of the major epaxial muscle segments of *Crotalus cerastes*. The thin anterior tendon (AT) of the SSP-SP extends posteriorly to end lateral to the tenth vertebra. The muscle tissue of the dorsomedial head (spinalis = SP) of the SSP-SP continues posteriorly for four more vertebrae. The muscle fibres then terminate on the posterior tendons of the segments of the M. multifidus, which extend posteriorly for less than two vertebrae and attach to the lateral surface of the neural spine. Thus, the resulting span of vertebrae for one segment of the SP is 15, including the vertebrae of origin and insertion. Muscle fibres from the ventrolateral head (semispinalis = SSP) of the SSP-SP attach directly to the fifteenth vertebra *via* a distinct ribbon-like tendon that is shared with the M. interarticularis superior.

Muscle tissue from a single segment of the LD extends anteriorly from its origin on the twenty-fifth vertebra to insert into a tendinous arch lateral to the twentieth vertebra of *C. cerastes*. The tendinous arch gives rise to a dorsomedial tendon (MT) that extends anterodorsally for three vertebrae and forms a diffuse attachment to the neural spines of the vertebrae (Fig. 2). The exact point of attachment of this medial tendon is difficult to determine because it becomes part of a connective tissue sheath surrounding the SSP-SP. The span of the LD from the prezygapophysial process to its rather indistinct dorsal attachment is nine vertebrae. The lateral tendon of the LD extends anteriorly for two vertebrae, whereupon a weak connection extends medially to the proximal portion of the rib. A more robust portion of this tendon extends ventrolaterally for an additional vertebra at which point the muscle fibres of the IC begin.

Fibres of the IC continue anteriorly for 11 vertebrae before terminating on a distinct tendon, slightly longer than a vertebra, that attaches to a rib. The IC of *C. cerastes* does not have a very distinct tendon between its medial and lateral heads. The span of the IC by itself is 14 vertebrae and with the associated LD segment is 21 vertebrae.

The major epaxial muscles of *Nerodia fasciata* and *Elaphe obsoleta* are more similar to each other than to those of *Crotalus cerastes*. The primary difference from *C. cerastes* is that in these two colubrids the medial tendon of the LD attaches to the SSP. In *N. fasciata* and *E. obsoleta* the muscle fibres of the SSP terminate on a tendinous sheet lateral to the vertebrae of insertion of the SP. Part of this tendinous sheet contributes to an intermuscular septum between the SSP-SP and LD. Another portion of the tendinous sheet extends ventrolaterally to form the medial tendon of the LD. In the spinalis head of the SSP-SP of *N. fasciata* the lengths of the anterior tendon, muscle tissue and total muscle span are 14, 5 and 20 vertebrae, respectively. In *E. obsoleta* these same lengths are 11, 5 and 18 vertebrae, respectively.

Muscle tissue from a single segment of the LD extends about six vertebrae anteriorly from its origin on the thirtieth vertebra of *N. fasciata* (and the twenty-seventh vertebra of *E. obsoleta*). In both *N. fasciata* and *E. obsoleta* the tendinous arch of the LD gives rise to a ventrolateral tendon that connects with the medial head of the M. iliocostalis in an arrangement similar to that of *C. cerastes*.

In contrast to the situation in *C. cerastes*, the medial and lateral heads of the IC of *N. fasciata* and *E. obsoleta* are divided by a distinct intermediate tendon about one vertebra long. The combined length of contractile tissue comprising both heads of the IC is about 10 vertebrae in both *N. fasciata* and *E. obsoleta*, in which 23 vertebrae are spanned by the interconnected segments of the LD and IC.

Deeper muscles occasionally implanted with electrodes included the Mm. multifidus (M), interarticularis superior (IAS) and interarticularis inferior (IAI). The M. multifidus is effectively identical in the three species (illustrated in Jayne, 1988). This triangular-shaped muscle lies deep below the SP. Anteriorly, the multifidus fibres form a wide attachment to the posterior portion of the postzygapophysial wing and these fibres taper posteriorly as they join a triangular tendon so that five vertebrae are spanned by a complete segment.

The IAS (M. digastricus of Mosauer, 1935) was occasionally implanted in *N. fasciata* and *E. obsoleta*, and it has a similar morphology in these two taxa (Jayne, 1988). Segments of this muscle originate from the posterior margin of the postzygapophysis just ventral to the fibres of the M. multifidus. As the fibres extend posteriorly, they bifurcate to form two distinct spindle-shaped heads. Each of these heads attaches to the posterior portion of the postzygapophysis *via* thin tendons about one vertebra long. Including the vertebrae of origin and insertion, four vertebrae are spanned by these segments.

The IAI lies deep below the LD of *E. obsoleta*. This muscle extends anteriorly four vertebrae from its origin on the prezygapophysial process to its insertion on the most proximal portion of a rib. Each segment receives some fibres from each of the vertebrae it spans.

The above abbreviations of muscles will be used to indicate the location of an electrode from which an EMG was obtained. In graphic summaries of results, the total spans of the muscle segments with implanted electrodes are given in parentheses after the muscle abbreviation. Muscle spans indicate the positions of the anteriormost and posteriormost vertebrae to which the muscle is attached, counting posteriorly from the skull. If an electrode was in more than one adjacent muscle segment, the span included the most anterior and posterior origins and insertions of all the contractile tissue of serial homologues containing the uninsulated electrode wire. Span of the IC of *N. fasciata* and *E. obsoleta* includes the associated segmental length of LD.

Sidewinding

Snakes perform sidewinding locomotion in either a left- or a right-handed manner. The following kinematic features characterize right-handed sidewinding (Figs 1, 3). The anteriormost portion of the snake is usually flexed (concave) to the

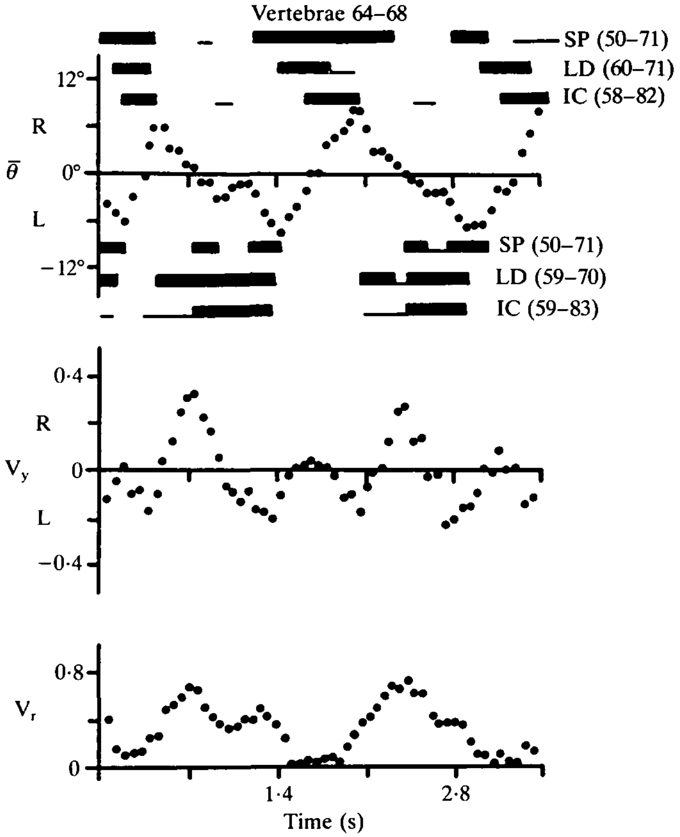

Fig. 3. Simultaneous EMG and movement records from *Nerodia* 36 performing two cycles of right-handed sidewinding on a linoleum floor. Right and left are abbreviated R and L. Numbers in parentheses after muscle abbreviations indicate the vertebrae spanned by the muscle segments containing the electrodes. Horizontal bars represent EMG, with thinner lines representing an amplitude about one-third that of the overall maximum for an electrode. EMGs of muscles from the right side of the snake are shown above the plot of $\bar{\theta}$, indicating lateral vertebral flexion concave to the right. V_r is overall speed and V_y is the lateral component of V_r. Velocities are in TL s^{-1} and are for the first vertebra (64) in the interval used to determine $\bar{\theta}$. The vertebral interval used to determine $\bar{\theta}$ was adjacent to the contractile tissue of the muscles containing the electrodes.

right. The left side of the snake pushes backwards against the substrate and often forms a windrow when the snake is on loose substrates such as sand. The plot of V_y *versus* time shows a pattern of left, right and left movement between times of static contact with the substrate (Jayne, 1986). The movements of left-handed sidewinding are mirror images of these.

Fig. 3 illustrates the simultaneous movement and EMG records of *Nerodia* 36 performing slightly more than two cycles of right-handed sidewinding. For the two periods between 0·31, 1·50 and 3·31 s, the values of mean V_x and coefficient of variation (CV) of V_r were 0·29 TL s^{-1}, 57 % and 0·25 TL s^{-1}, 79 %, respectively. Allowing for the error of digitizing, static contact with the substrate was from 1·50 to 1·88 s and from 3·13 to 3·31 s. Fig. 3 includes the activities of left and right segments of SP, LD and IC near the midbody of the snake. Fig. 4 illustrates sample EMGs of these six muscles during the interval from 0·55 to 2·50 s of this same sequence.

For this sequence in *Nerodia*, most of the major muscle activity correlated with lateral flexion of the vertebrae towards the side of the active muscles. The major activity of the IC was unilateral over the entire duration of the illustrated sequence

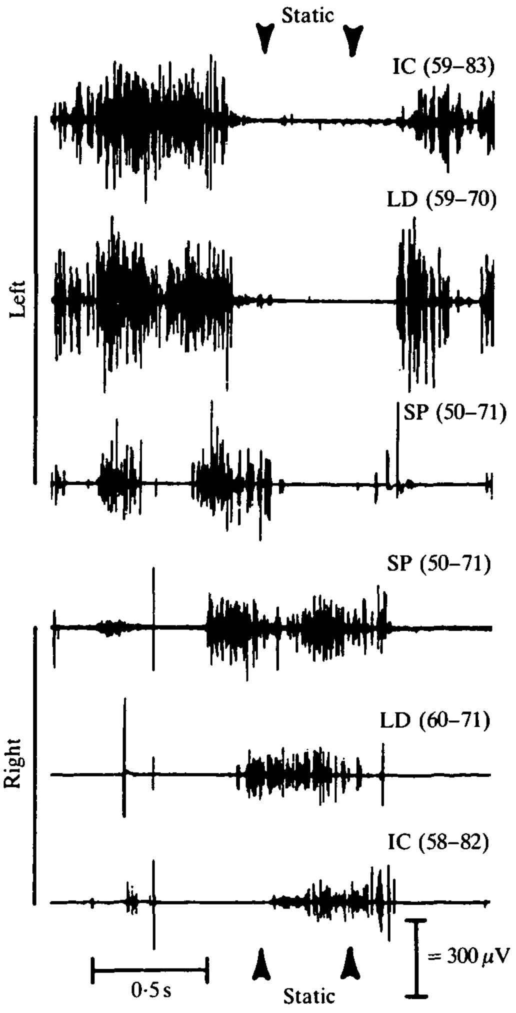

Fig. 4. Sample EMGs from 0·55 to 2·50 s during the sidewinding of *Nerodia* 36 (Fig. 3): EMGs from the left and right side are shown. Horizontal and vertical bars indicate time and voltage scales, respectively. The vertical bar = 400 μV for the right LD and IC. Arrowheads indicate beginning and end of static contact. Note bilateral activity of the SP and that the beginning of strong activity of the IC lags behind that of the LD.

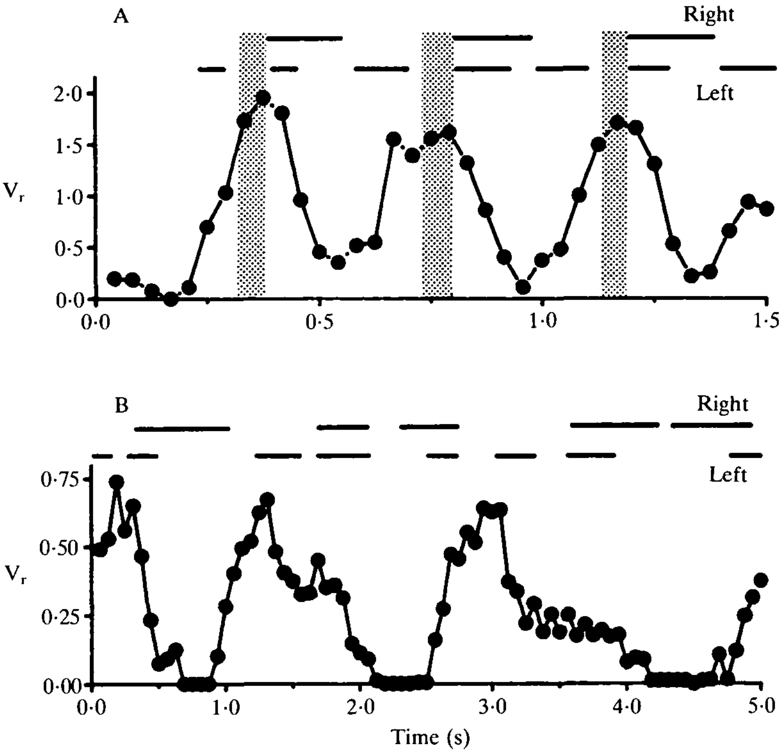

Fig. 5. Midbody spinalis (vertebra 66) activity during the right-handed sidewinding of *Nerodia* 36. Note the difference in the timing of bilateral activity with respect to static contact (or minimum V_r) between A and B. (A) A relatively fast sequence of sidewinding. The stippled regions indicating times lacking any activity at midbody of right and left segments of the SP, LD and IC. (B) For this slower sequence of sidewinding, there was no time during which at least one of the right or left midbody SP, LD or IC segments was not active.

(Fig. 3). With the exception of overlap from 0·09 to 0·13 s, the major activity of the LD segments was also unilateral. Major activity of the right SP consistently began before that of the right LD and IC, and this time of activity overlapped with that of the left SP (Figs 3, 4). To a lesser extent, major activity of the left SP and right LD also overlapped. Activity of the left LD and IC ceased slightly prior (about 0·1 s) to static contact, whereas activity of the left SP ceased almost exactly at the initiation of static contact with the substrate. This suggests that bilateral contractions of the SP elevated the region of the body posterior to the area of static contact. Some weak activity of the right SP and IC correlated with a slight straightening of the body about midway through the transition from concave right to concave left.

Some differences in the timing of spinalis activity in *Nerodia* appear to be correlated with changes in speed. Fig. 5 illustrates the activity of the left and right midbody spinalis segments for two additional sequences. Mean V_x for each of the three periods of motion shown in Fig. 5A ranged from 0·68 to 0·77 TL s^{-1}. V_r was not quite equal to zero early in this sequence because of some backward slipping of the snake. The bilateral activity of the spinalis segments at midbody always preceded the time of static contact (or minimum V_r). Another interesting feature of this fastest sequence of *Nerodia* was the occurrence of about 0·06 s of total inactivity of the left and right midbody SP, LD and IC segments. This inactivity was correlated with maximal V_r (see stippled area of Fig. 5A) and implies that momentum may be sustaining movement at higher speeds. During the slower sequences of sidewinding, at least one of the right or left midbody SP, LD or IC muscles was active at any given time (Figs 3 and 4).

Fig. 5B illustrates the synchronous records of V_r and midbody spinalis activity for a slower sequence of right-handed sidewinding. Mean V_x values for the first and second complete periods of motion were 0·23 and 0·21 TL s^{-1}, respectively. The first time of bilateral spinalis activity (from 0·30 to 0·49 s) occurred before static contact. For the remainder of the sequence bilateral spinalis activity both preceded and followed static contact. The right spinalis activity shown in Fig. 5B (unlike that in Fig. 5A) became biphasic with momentary inactivity (lasting 0·28 and 0·13 s) about midway through the second and third times of static contact.

To allow pooling of data obtained from sequences of different speeds, seven times of onset and cessation of each muscle's activity were converted to a standardized cycle of movement where the initiation of static contact occurred at 0 % and the end of a cycle was 100 %. Fig. 6 summarizes these relative times of midbody muscle activity during the sidewinding of *Nerodia*. One-way ANOVA revealed no significant differences among the relative times of the onset of left-side activity and offset of right-side activity ($P = 0{\cdot}94$). One-way ANOVA of the offset of left-side and the onset of right-side activity revealed highly significant differences among muscles ($P = 0{\cdot}002$). Tukey's procedure indicated that offset of the left SP was significantly ($P < 0{\cdot}05$) later than both onset of the right SP and offset of the left IC activity. Furthermore, the relative time of onset of the right IC occurred significantly later than both the onset of the right SP and the offset of the left IC.

To summarize, during right-handed sidewinding of *Nerodia* the right-side muscles were active as a collective group before, during and after static contact, as the vertebrae flexed from maximally convex to maximally concave to the right (Fig. 6). In contrast, the left-side muscles were primarily active between times of static contact, as the vertebrae flexed from maximally convex to maximally concave to the left. Bilateral activity of the SP immediately preceded or followed static contact as the body was elevated.

Fig. 7 illustrates two periods of motion and simultaneous muscle activity of *Crotalus* 6 performing right-handed sidewinding on sand. For the period of movement from 0·31 to 1·54 s, mean V_x and CV of V_r were 0·49 TL s^{-1} and 78 %, respectively. Strong activity of the right SP began just before static contact when the region was still convex to the right and continued until the region was maximally concave to the right, whereupon weaker activity continued until the

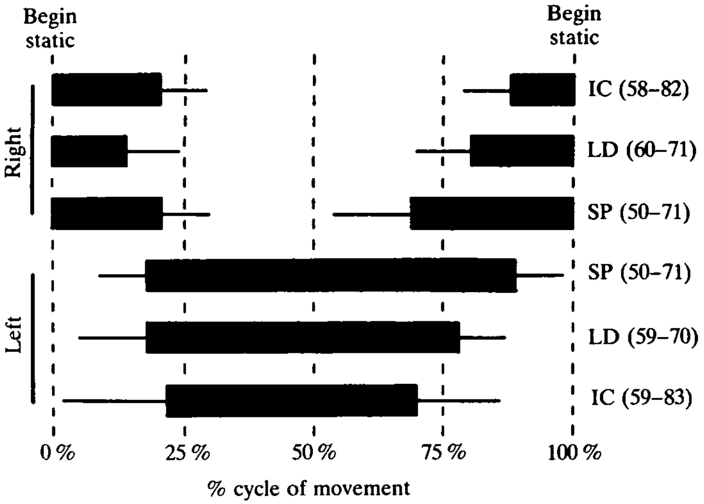

Fig. 6. Mean relative times of activity calculated from seven simultaneous recordings of six midbody muscles during the right-handed sidewinding of *Nerodia*. The ends of the thick horizontal bars indicate the mean times of onset and offset of activity and the thin bars represent ± one standard deviation. The initiation of static contact occurs at 0 % of this standardized cycle of a movement. Flexion to the left occurs about from 20 % to 80 %. The top three muscles are on the right side of the snake and the others are from the left side. Note that activity of the SP was occasionally discontinuous.

region was almost straight. The major activity of the left M began when the vertebrae were maximally convex to the left and continued until the vertebrae were almost straight. Some weak activity of the left M occurred just prior to static contact with the substrate.

Crotalus 6 also performed left-handed sidewinding, for which synchronous movement and EMG records are illustrated in Fig. 8. For vertebra 51, during the complete period of movement from 0·29 to 1·21 s, values for mean V_x and CV of V_r were 0·67 TL/s^{-1} and 64 %, respectively. EMGs were obtained from both the right SP and left M at vertebra 51 and from the left LD at vertebra 81. Both the left muscles were active before, during and after static contact as the vertebrae flexed from maximally convex to maximally concave to the left. The major activity of the right SP began well after static contact while the vertebrae were maximally convex to the right and ceased as this region became straight. Lesser activity of the right SP began almost exactly when static contact was initiated and ceased slightly after static contact.

The lag between these two sites at vertebrae 51 and 81 (Fig. 8) illustrates the posterior propagation of EMG and mechanical events. Lag times between sites 1 and 2 for the first and second times of static contact were 0·43 and 0·42 s, respectively. The overlap in activity of the left-side muscles from the two sites suggests that more than 30 adjacent muscle segments may be active simultaneously.

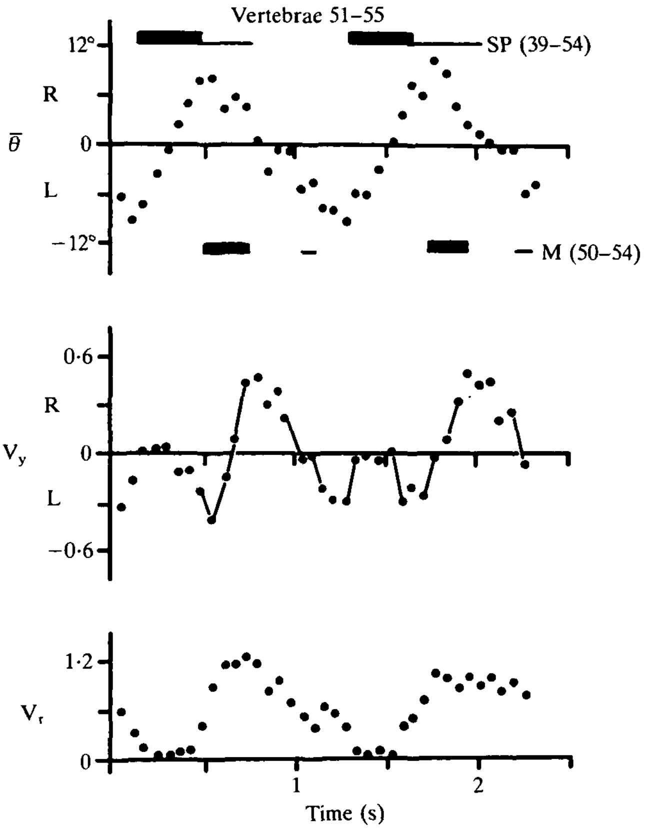

Fig. 7. Simultaneous EMG and movement records for *Crotalus* 6 performing right-handed sidewinding on sand. Notation is as in Fig. 3.

Another *Crotalus* (5) also performed both left- and right-handed sidewinding while moving on sand. An electrode site at the 88th vertebra of this snake included the left and right SP and IC and the right LD. Activity of the left and right IC did not overlap during either left- or right-handed sidewinding. The greatest overlap of major activity occurred between the left and right SP during both left- and right-handed sidewinding. This time of bilateral SP activity began just after static contact when the vertebrae were being flexed and lifted away from the substrate. To a lesser extent, the LD could also be active during this period of bilateral SP activity. Activity of the SP during the lifting phase occurred either as a continuation of earlier activity (as seen in Fig. 7) or as a distinct second contraction. As the vertebrae were being flexed to the right during right-handed sidewinding, the onset of activity of the right IC often lagged slightly behind that of the right SP and LD.

Fig. 9 summarizes the muscular mechanism of left-handed sidewinding of *Crotalus cerastes*. During left-handed sidewinding, unilateral activity of the left-side muscles (SSP-SP, LD and IC) flexed the vertebrae to the left as they move

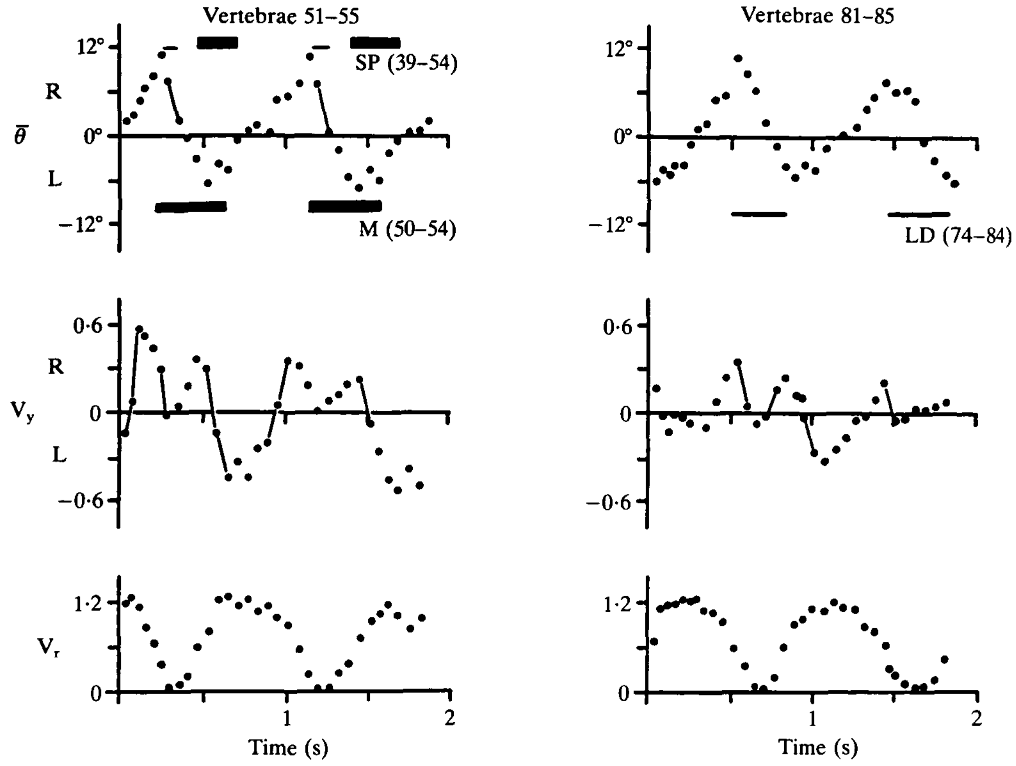

Fig. 8. Simultaneous EMG and movement records for two sites in *Crotalus* 6 performing left-handed sidewinding on sand. Notation is as in Fig. 3.

anteriorly towards a region of static contact. Left-side activity of these muscles continued through and beyond static contact until the vertebrae were maximally flexed to the left. Right-side activity (SSP-SP, M and some LD) began during or just after static contact with the substrate. Right-side activity (including IC) continued at least until the vertebrae began to flex to the right. Depending on the exact posture of the snake, right-side activity could continue until the region was maximally concave to the right. This continuation of right-side activity was more likely when the region approaching static contact was not flexed very tightly to the right. Bilateral activity (primarily of the SSP-SP and M) lifted the body near areas of static contact. Right-handed sidewinding can be described by switching left and right in the above description.

In both left- and right-handed sidewinding, the muscles primarily had unilateral, posteriorly propagated contractions from maximal convexity to maximal concavity of the vertebrae. Bilateral activity occurred during the lifting phase.

Concertina locomotion

Fig. 10 shows synchronous EMG and movement records of *Nerodia* 33 performing concertina locomotion in an 8 cm wide tunnel. This sequence includes three

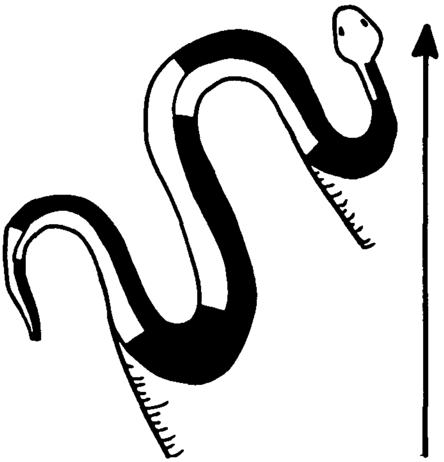

Fig. 9. Summary of the muscular mechanism of left-handed sidewinding of *Crotalus cerastes*. Shaded regions indicate active contractile tissue of either the SSP-SP, LD or IC. The arrow indicates the overall direction of travel of the snake, and former regions of static contact are indicated as the tracks left behind the snake. Regions of muscle activity are propagated posteriorly; hence, the posterior and anterior margins of these regions represent onset and offset, respectively. See text for more detailed description.

complete cycles of activity between 0·33, 2·98, 4·82 and 7·10 s and mean V_x of these periods was 0·06, 0·08 and 0·06 TL s^{-1}, respectively. Static contact with the substrate was about 0·5 s for each of these periods, causing an expectedly high CV value of V_r (90 %) from 0·33 to 7·10 s. As indicated by a comparison of V_y and V_r profiles, the lateral excursions of this region of the snake were usually very slow. The pattern of motion of concertina locomotion (Jayne, 1986) can vary widely, as is shown in Fig. 10. From the first to second time of static contact, vertebrae 70–74 of the snake were concave right, concave left and then straight. During the second cycle of motion, this region of the snake was straight, concave right, concave left and briefly concave right before remaining concave left. During the third cycle, these vertebrae changed from concave left to concave right. The pattern of muscle activity was correspondingly variable within a cycle of motion. No major muscle activity was bilateral, although some weak bilateral activity occurred occasionally. Furthermore, most EMGs correlated with lateral vertebral flexion towards the side of the contracting muscle. Muscle activity not correlated with these angular accelerations occurred on the concave sides of the snake during static contact with the sides of the tunnel (e.g. from 7 to 8 s). For this sequence, right-side muscle activity maintained contact with the sides of the tunnel during the first, second and fourth times of static contact, and left-side activity occurred during the third static contact (Fig. 10).

Fig. 11 illustrates simultaneous EMG and movement records for two sites of *Elaphe* 15 performing concertina locomotion in an 8 cm wide tunnel. For vertebra

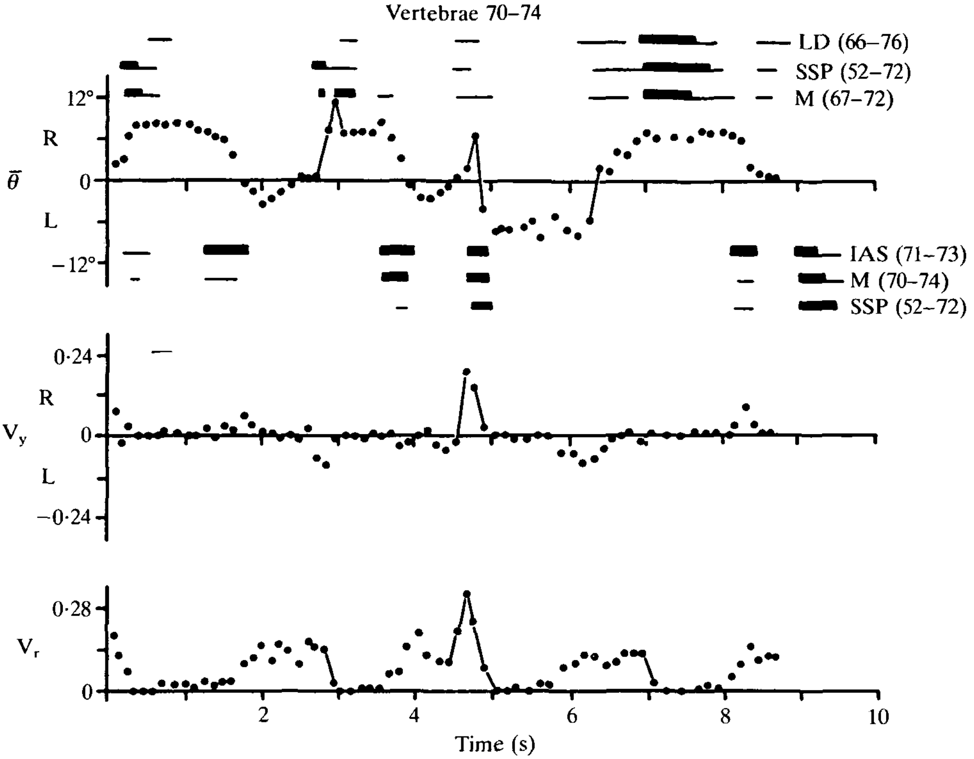

Fig. 10. Simultaneous EMG and movement records from *Nerodia* 33 performing concertina locomotion in an 8 cm wide tunnel. Notation is as in Fig. 3.

133, means of V_x for the two periods occurring between 0·87, 3·40 and 5·83 s were 0·04 and 0·06 TL s^{-1}, respectively. The value for CV of V_r was 81 % for the time interval containing these two cycles, and the durations of the three times of static contact with the substrate were about 0·5, 0·5 and 0·3 s, respectively. The electrodes at sites 1 and 2 were in contractile tissue at the 110th and 130th vertebrae, respectively. For both these sites, movement records are shown for three vertebral intervals within the span of the muscle segments from which EMGs were recorded. As discussed earlier, the contractile tissue of a SSP-SP muscle segment spans only about five vertebrae beginning about two vertebrae anterior to the origin of fibres on the tendon of the M. multifidus. As shown in Fig. 10, the most consistent mechanical correlate of EMGs occurred in the region spanned by the contractile-tissue portions of the muscle segments. In fact, the vertebrae adjacent to the most anterior portion of the anterior tendon of the SSP-SP may undergo flexion opposite to the direction expected for left-side muscle activity (e.g. time 0–0·5 s for vertebrae 121–125). In the region of contractile tissue, activity could occur while the region remained convex (first and second EMGs, vertebrae 109–113, Fig. 11A) or while it remained concave (first and second

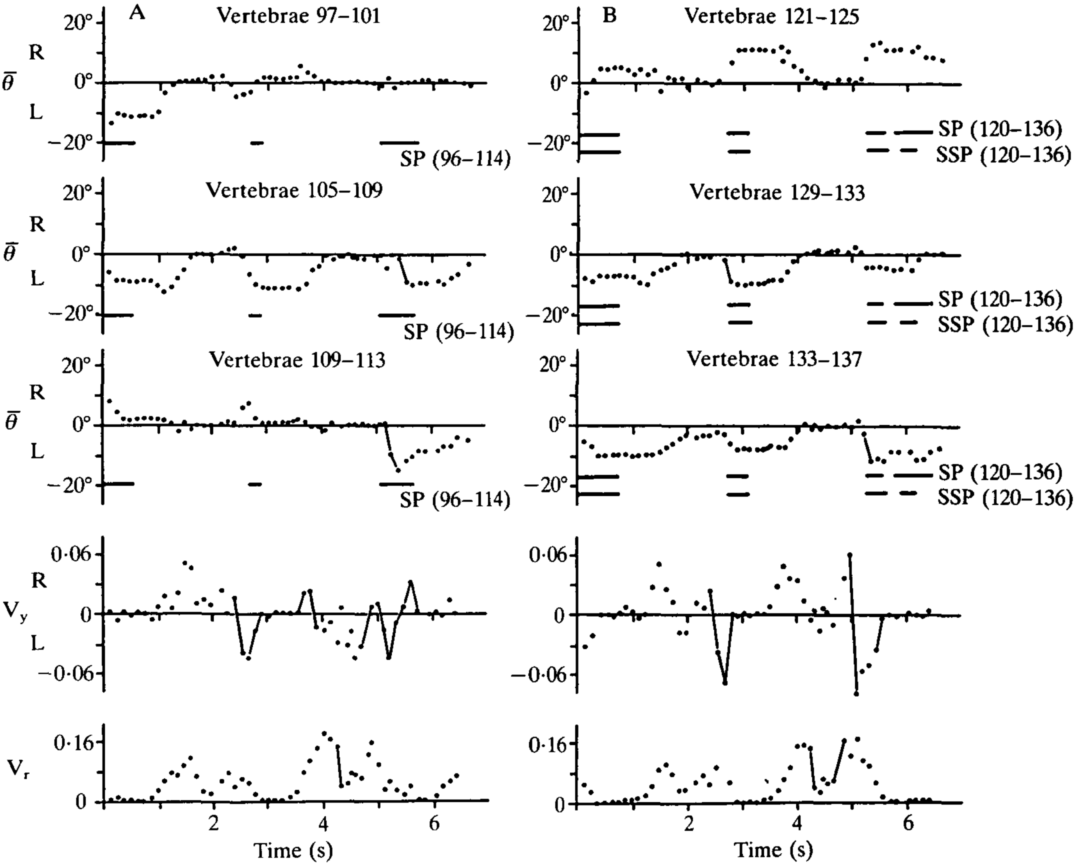

Fig. 11. Simultaneous EMG and movement records for two electrode sites of *Elaphe* 15 performing concertina locomotion in an 8 cm tunnel. For each set of EMGs, $\bar{\theta}$ is shown for three vertebral regions within the span of the muscle segments. Note that more anterior vertebrae (farthest away from the contractile tissue) do not have patterns of vertebral flexion that consistently correlate with muscle activity. Linear velocities are shown for vertebrae 109 (A) and 133 (B).

EMGs, vertebrae 133–137, Fig 11B); however, muscle activity in these regions always correlated with vertebral flexion towards the side of activity or with the maintenance of a concave posture during static contact.

To clarify the sequence of muscle activity and mechanical events occurring along the length of snakes performing concertina locomotion, six electrodes were implanted at regularly spaced intervals along a single side of each of three snakes. Fig. 12 illustrates the synchronous records of muscle activity and vertebral flexion for six sites spaced at 10-vertebra intervals in *Nerodia* 40 performing concertina locomotion in a 5 cm wide tunnel. Rather than a constant lag occurring between successive sites, neither the muscle activity nor the pattern of lateral vertebral flexion is propagated posteriorly in a simple continuous fashion (Fig. 12). Records

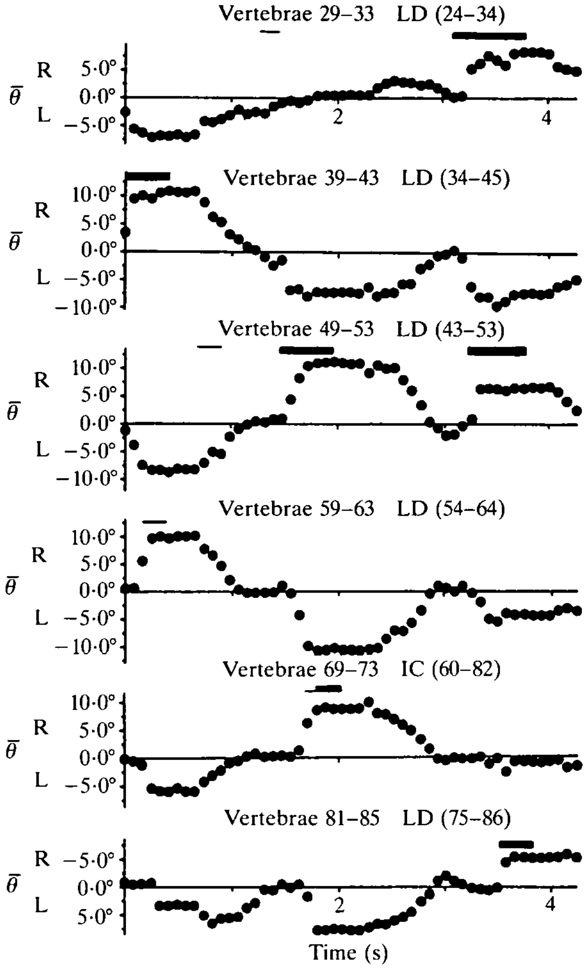

Fig. 12. Simultaneous EMG and vertebral flexion records for six longitudinal electrode sites, spaced at 10-vertebra intervals along the right side of *Nerodia* 40 performing concertina locomotion in a 5 cm wide tunnel. Note the lack of a constant lag in either the mechanical event (vertebral flexion) or the muscle activity between successive sites.

from electrodes placed at 10- and 20-vertebra intervals in two *Elaphe* also lacked a constant lag during concertina locomotion.

Sites of static contact with the sides of the tunnel are established from anterior to posterior; however, this is accomplished by alternating regions of left and right muscle activity that flex the vertebrae laterally until and slightly after the sides of the tunnel are touched. The entire sequence of events following the initial anterior static contact depends on tunnel width, snake length and the distance along the snake from the initial site of static contact. The location of the first region of static contact is variable and unpredictable. Consequently, the patterns of muscle

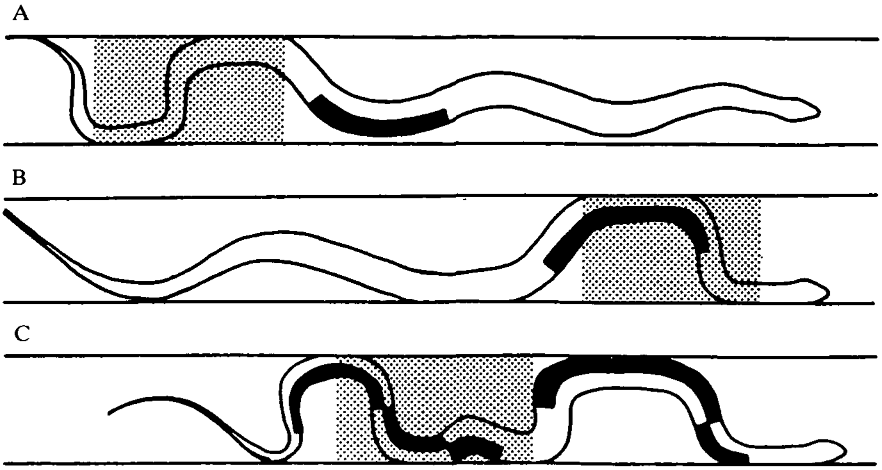

Fig. 13. Summary of the muscular mechanism of concertina locomotion. Images were traced from films of a *Nerodia* (TL = 100cm) moving in a 10 cm wide tunnel. Shaded regions within the outline of the snake indicate regions of active contractile tissue, and stippled areas indicate static contact between the snake and the substrate. The progression of events is from A to C.

activity and vertebral flexion at any given site in the snake will be correspondingly variable. Hence, a constant lag of events will not be observed over several cycles of activity.

Fig. 13 summarizes the muscular mechanism of concertina locomotion. Although this figure is based on tracings made of a *Nerodia* (TL = 100 cm) moving through a 10 cm wide tunnel, the relationship of muscle activity to vertebral flexion and areas of static contact can be generalized for all observed snakes and tunnel widths. Shaded areas within the outline of the snake indicate active muscles. It is important to remember that these blocks of active muscle segments were not propagated posteriorly in a continuous fashion as were those shown in Fig. 9. In Fig. 13A the snake was just about to cease static contact with the substrate in its posterior region and the right-side muscle activity involved in straightening the body was just about to end. In Fig. 13B the snake now had well-established regions of static contact with the right (most anterior) and left (second-most anterior) sides of the tunnel. Right-side muscle activity flexed the vertebrae to the right and the snake was about to establish a third region of static contact, with the right side of the tunnel. At a time between Fig. 13B and Fig. 13C there were momentarily four regions of static contact with the sides of the tunnel. Proceeding from anterior to posterior these regions of contact were on the right, left, right and left sides of the snake. Fig. 13C shows the snake just as it was discontinuing static contact in the two most anterior regions, where muscle activity was beginning to straighten the body. More posteriorly there was a region of no muscle activity during the final phase of static contact and just before straightening of the body would commence. A more posterior region of the snake in Fig. 13C had muscle activity which was maintaining the vertebrae in a flexed position that perpetuated static contact. Finally, the most posterior muscle activity was flexing the vertebrae to the right.

Depending on the longitudinal position within a snake and the size of the snake relative to the tunnel, it was apparently not uncommon for some regions to be straightened passively as they were pulled forward towards a region of static contact (Fig. 12). Almost without exception, flexion of the vertebrae from straight to concave was the result of muscle activity (Figs 10–12).

In summary, concertina locomotion in tunnels was performed by snakes using alternating, unilateral muscle contractions. Muscle activity could occur when a region was convex, concave or undergoing the transition from convex to concave. EMGs were either correlated with lateral vertebral flexion towards the side of activity or were associated with the maintenance of a concave posture during static contact with the sides of the tunnel.

Effect of tunnel width on concertina locomotion

To clarify the interactions between snake size and tunnel width, four cycles of activity were analysed for both a *Nerodia* 40 and an *Elaphe* 21 performing concertina locomotion in tunnels 5, 7·5 and 10 cm wide while electrodes, implanted at 10-vertebra intervals, monitored activity of the right-side muscles. Table 2 summarizes the mean values of the measured kinematic and electromyographic variables. For each of the first 10 variables in Table 2, a two-way ANOVA (using each of the four measurement per snake per tunnel width) was performed to determine significant differences ($P < 0{\cdot}05$) between the *Nerodia* and *Elaphe* and among the three tunnel widths. A similar two- way ANOVA was used for $\mathrm{EMG}_{\mathrm{max}}$ using the 4–6 observed values per snake per tunnel.

Duration of movement and total duration of a cycle were significantly different between the *Nerodia* and the *Elaphe*. Duration of static contact per cycle varied significantly between *Nerodia* and *Elaphe* and among the different tunnel widths. The mean absolute forward velocity (V_{cm}) showed no significant differences among the treatments whereas the mean relative forward velocity (V_{tl}) varied significantly between *Nerodia* and *Elaphe*. As expected, the minimum number of vertebrae between left and right regions of static contact increased significantly with increasing tunnel width as well as being significantly different between *Nerodia* and *Elaphe*. The number of lateral regions of static contact increased significantly as tunnel width decreased. The forward movement per cycle (Δx) and the mean angle of the snake relative to the tunnel ($\bar{\alpha}$) both increased significantly with tunnel width and were different between *Nerodia* and *Elaphe*. Δx also had a significant interaction term between tunnel width and the two different snakes. Maximal vertebral flexion varied significantly only with tunnel width. Maximum duration of major muscle activity varied significantly between *Nerodia* and *Elaphe* and among the different tunnel widths. Although no tests of significance were performed on the estimates of maximum number of simultaneously active adjacent muscle segments, this quantity generally increased with increasing tunnel width and was often greater for the *Elaphe* than the *Nerodia* in a given tunnel. It appears

Table 2. *Mean kinematic and electromyographic measurements for the concertina locomotion of a* Nerodia *(TL = 100 cm) and an* Elaphe *(TL = 159 cm) in 5, 7·5 and 10 cm wide tunnels*

Snake (tunnel)		T_s	T_m	T_t	Δx	V_{cm}	V_{tl}	$\bar{\alpha}$	$\bar{\theta}_{max}$	N_{static}	Vert.	Seg-ments	EMG_{max}
Nerodia	Mean	0·69	1·20	1·89	12·3	6·6	0·066	43·8°	14·8°	10·5	5·8	<10	0·54
(5 cm)	Range	0·56–0·94	1·00–1·31	1·56–2·24	10·7–13·8	5·7–7·4	0·057–0·074	43·4–44·2°	12·5–16·0°	9–12	5–6		0·31–0·71
Nerodia	Mean	0·83	1·46	2·29	10·9	5·0	0·050	64·0°	13·4°	5·8	11·3	>10	0·61
(7·5 cm)	Range	0·67–1·08	0·92–1·46	1·57–3·16	9·8–12·9	4·1–6·6	0·041–0·066	56·3–68·3°	13·0–14·0°	5–6	10–12		0·20–0·90
Nerodia	Mean	1·15	1·54	2·69	18·1	7·2	0·072	90·0°	14·5°	3·8	15·0	>30	0·72
(10 cm)	Range	0·42–2·16	1·33–1·75	1·75–3·49	15·4–19·4	5·5–10·6	0·055–0·106	88·3–92·0°	14·0–15·0°	3–4	14–16		0·48–1·01
Elaphe	Mean	1·31	1·78	3·19	15·7	5·4	0·034	53·8°	13·8°	8·8	9	>20	0·90
(5 cm)	Range	1·00–1·62	1·00–2·12	2·00–3·74	12·8–18·2	3·5–7·2	0·022–0·045	51·3–58·3°	11·5–15·0°	8–10	8–10		0·73–1·53
Elaphe	Mean	1·46	2·16	3·62	21·9	4·5	0·028	79·2°	14·3°	6·5	14·3	>20	1·39
(7·5 cm)	Range	1·14–1·88	1·56–2·92	2·81–4·48	19·3–24·3	4·6–6·9	0·029–0·043	71·4–89·0°	8·5–14·5°	6–7	14–15		1·00–1·87
Elaphe	Mean	1·50	3·28	4·78	28·7	6·9	0·043	101·6°	14·3°	4·8	18·3	>30	1·29
(10 cm)	Range	0·75–2·00	1·75–4·58	2·50–7·08	23·6–36·0	4·0–10·7	0·067–0·025	89·0–114·5°	13·0–16·0°	3–6	17–20		1·15–1·50

T_s, T_m and T_t are durations of static contact, moving and total per cycle (to the nearest 0·01 s).

Δx, V_{cm} and V_{tl} are forward movement (cm) and average forward velocities (cm s^{-1} and TL s^{-1}) for each cycle of movement.

$\bar{\alpha}$ is the mean of the angles between the tunnel and the body of the snake between regions of static contact during one cycle.

$\bar{\theta}_{max}$ is maximal vertebral flexion, averaged for two adjacent vertebral joints.

N_{static} is the maximum number of simultaneous regions of lateral static contact.

Vert. is minimum number of vertebrae between sides of the tunnel.

Means of all the preceding variables had a sample size of four.

Segments is the estimated number of simultaneously active adjacent muscle segments.

EMG_{max} (in s) is the maximum duration of major continuous activity observed for each muscle for each tunnel width ($N = 4$–6).

See text for more detail.

that the different relative forward velocities of the *Elaphe* and *Nerodia* are correlated with the observed differences in $\mathrm{EMG_{max}}$. V_{tl} of the *Elaphe* was about half that of the *Nerodia*, and there was about a twofold difference in the values of $\mathrm{EMG_{max}}$ of these two snakes.

Discussion

Sidewinding

The electromyographic event most characteristic of sidewinding is bilateral activity of the spinalis (SP). Figs 2–7 illustrate the EMG records during the sidewinding of these two species. Both species had substantial bilateral activity of the SP. The multifidus of *Crotalus* also overlapped strongly with the SP and M of the opposite side (no EMGs were obtained from the M of *Nerodia*). In both species the bilateral activity correlated with a time when lifting of the vertebrae was occurring. The lifting phase (bilateral activity) of *Nerodia* could occur either before or after static contact whereas that of *Crotalus* occurred after static contact. Hence the range in the motor pattern of sidewinding observed in *Nerodia* encompassed the pattern observed in *Crotalus* despite the different substrates used in the experiments.

This activity of the SP corresponds closely to the recent suggestions of Fetcho (1986, 1987), who examined the organization of the motoneurones of the axial muscles of *Nerodia fasciata pictiventris* and discussed the general patterns of axial muscle motoneurones in vertebrates. After labelling nerves with horseradish peroxidase, Fetcho (1986) found that within the spinal cord the motoneurones of the SSP-SP showed a high degree of transverse spatial segregation compared with those of both the LD and the IC, whereas the location of the motoneurones of the LD and IC overlapped considerably. Another conspicuous feature of the motoneurones of the SSP-SP was that they had dendrites crossing to the opposite sides of the spinal cord. The spatial segregation of motoneurones appears to be a common feature of muscles with different times of activity, and the contralateral connection of motoneurones may be a trait of muscles that display bilaterally synchronous activity (Fetcho, 1987). The EMGs obtained from sidewinding snakes (Fig. 4) clearly indicate that activity of the SSP-SP can be independent of that of the LD and IC and that there is also much synchronous bilateral activity of the SSP-SP.

Although sidewinding is often considered to be somewhat specialized, it occurs in a wide variety of taxa including booid and colubroid snakes (Gans & Mendelssohn, 1972), but it is best documented for colubroids. The viperid *Crotalus cerastes* and the colubrid *Nerodia fasciata* belong to two distinct lineages of snakes and they both sidewind, although *C. cerastes* appears to be considerably more proficient at this mode than *N. fasciata* (Jayne, 1986). *Nerodia* needs to be encouraged to elicit sidewinding, and it is most easily elicited from small individuals. For larger *Nerodia*, it was more difficult to prompt good sidewinding on sand. For this reason, individuals were placed on the floor to obtain film of this

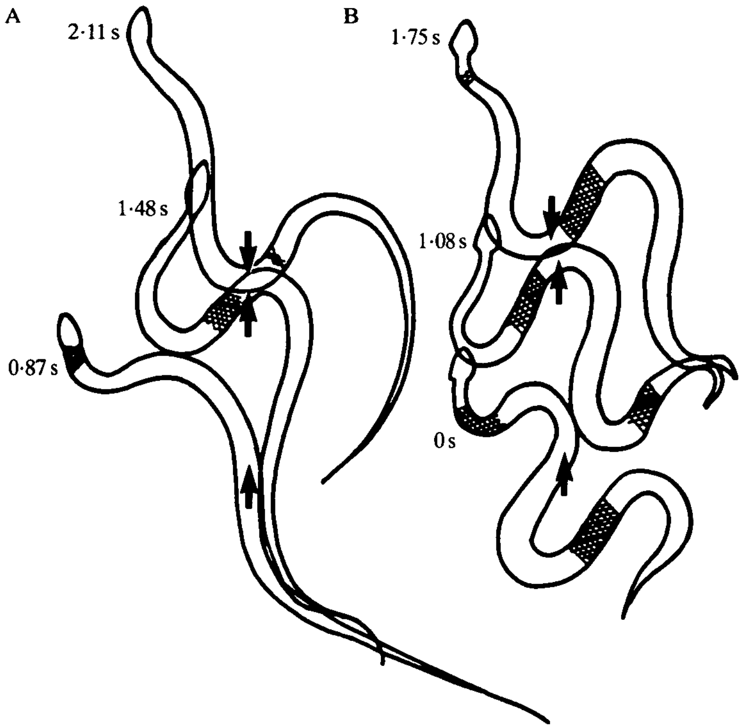

Fig. 14. Representative postures of snakes performing sidewinding. Illustrations were made from tracings of films. Cross-hatched regions indicate static contact with the substrate. Arrows are at vertebra 70. (A) From *Nerodia* on a linoleum floor (Figs 3 and 4). (B) Tracings from films of *Crotalus* 5 on sand. See discussion for more complete explanation.

mode, and the kinematic profiles of the larger *Nerodia* observed in this study appeared nearly identical to those of the smaller *Nerodia* crawling on sand in the study of Jayne (1986). Although no films were taken of *C. cerastes* sidewinding on the floor, individuals were allowed to crawl on the floor, and they readily performed sidewinding which appeared no different from that performed on sand. Allowing for the different substrates, it is still instructive to compare the sidewinding of these two species.

The patterns of muscle activity were often very similar in *N. fasciata* and *C. cerastes* during this study; however, some subtle postural differences were observed. Jayne (1986) discussed a significant difference between *N. fasciata* and *C. cerastes* for the angle of the track of static contact relative to the overall direction of travel. This difference implied that the posture of *C. cerastes* facilitated a greater area of the body having static contact with the substrate. Fig. 14 illustrates the postures during sidewinding from which EMGs were obtained. Fig. 14A illustrates the posture of *Nerodia* on a linoleum floor. This snake usually had only one region of static contact with the substrate. At 0·83 s, the *Nerodia* was establishing static contact between the neck and the substrate just after a brief period of backward sliding. At 1·48 s, it had a well-established region of static contact near mid-body. At 2·11 s the snake had lost static contact near mid-body and would soon establish static contact with the neck region. Interestingly, the portion of the snake posterior to about the 100th vertebra never established static contact.

This posture of *Nerodia* differed from that of the *C. cerastes* shown in Fig. 14B. At 0 s the *Crotalus* had firmly established static contact with the neck region while a more posterior region was also in static contact. At 1·08 s, the snake had two well-established, parallel regions of static contact. At 1·75 s, the snake was just beginning to contact the substrate with its neck, while it continued to maintain a large posterior region of static contact. Thus, during the conditions of this study, the *Nerodia* tended to pivot about a single region of static contact, whereas the *Crotalus* moved its body between two extensive regions of static contact. Furthermore, *Crotalus* used a greater percentage of its total length to establish static contact, in comparison with *Nerodia*.

Concertina locomotion

A unique feature of concertina locomotion is the absence of the continuous posteriorly propagated wave of muscle activity that was observed in terrestrial and aquatic lateral undulation (Jayne, 1988) and sidewinding. Furthermore, there is a highly variable pattern of movement and muscular activity within a single region of the snake with time. These traits suggest that muscle activity may occur in response to the changing location within a snake that first establishes static contact.

As indicated previously, not all the differences in concertina locomotion are solely the result of the variable location of the first region of static contact. There were also significant effects attributable to the width of the tunnel and the species of snake. Fig. 15 illustrates some of the postural differences that occurred for different tunnel widths used by *Nerodia* and *Elaphe*. The angle formed between the tunnel and the portion of the snake's body between regions of static contact increased with increased tunnel width and was greater for *Elaphe* than *Nerodia* within any tunnel width (Table 2; Fig. 15). Interestingly, the maximal vertebral flexion did not vary between these two snakes. Perhaps this indicates that a region posterior to an area of static contact with the side of the tunnel is maximally flexed until the opposite side of the tunnel is contacted. Consequently, the observed angle of the body relative to the tunnel results more from the different numbers of vertebrae that can fit between the sides of the tunnel than from different flexion per joint.

A simple model of concertina locomotion can be generated to quantify some of the effects of posture of the snake within a tunnel and the relative size of the tunnel. Fig. 16A illustrates a hypothetical length of snake touching the right and left sides of a tunnel at points *a* and *b*. The snake has a maximum diameter, D. One may assume that the forward progression of the snake (Δx_i) is the result of simple straightening of the vertebral column at points *a* and *b* while static contact is

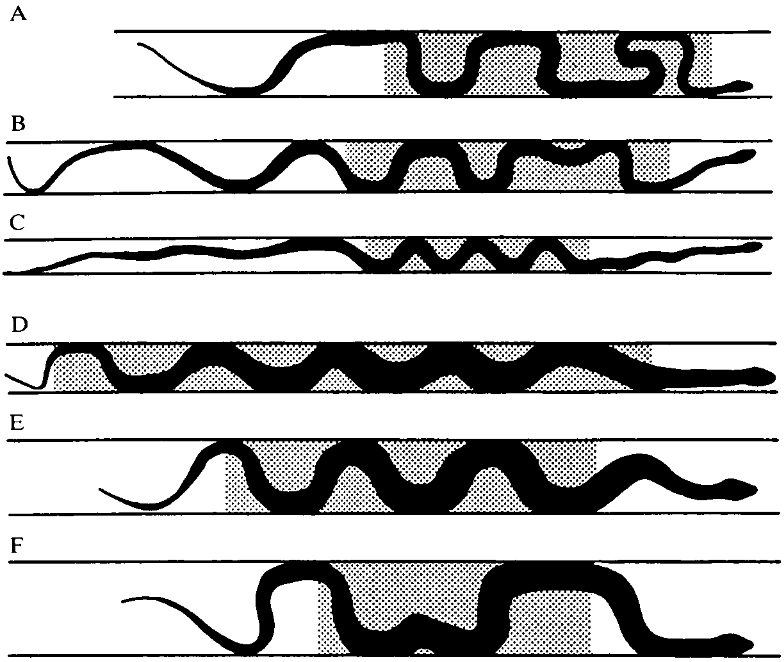

Fig. 15. Postural differences between *Elaphe* and *Nerodia* performing concertina locomotion in tunnels of varying width. Areas of static contact are indicated by the stippled areas. (A–C) Tracings from films of an *Elaphe* (TL = 159 cm) moving through 10 (A), 7·5 (B) and 5 (C) cm wide tunnels. (D–F) Tracings from films of a *Nerodia* (TL = 100 cm) moving through 5 (D), 7·5 (E) and 10 (F) cm wide tunnels.

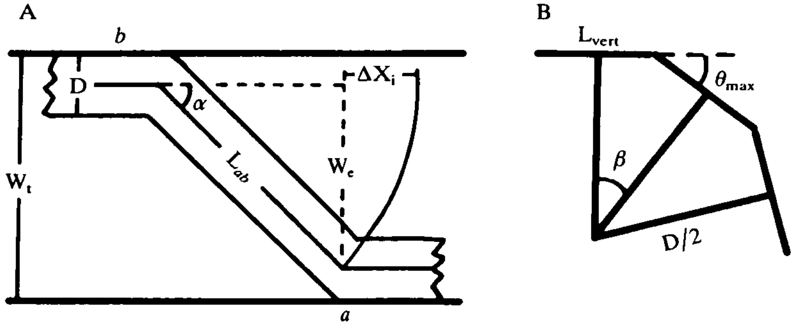

Fig. 16. Schematic representations of posture within a tunnel during concertina locomotion (A) and of maximally flexed vertebrae (B). See Discussion for complete explanation.

maintained at point *b*. The tunnel has width W_t, but when considering vertebral movements, the effective tunnel width, W_e, is equal to the difference between W_t and D. The length of the vertebral column between points *a* and *b* is L_{ab} and this portion of the snake forms an angle, α, relative to the sides of the tunnel. Solving for the movement resulting from complete straightening of the vertebral column:

$$\Delta x_i = L_{ab} - L_{ab}(\cos\alpha), \tag{1}$$

$$= L_{ab}(1-\cos\alpha) \tag{2}$$

After substituting for L_{ab}:

$$\Delta x_i = W_e(1-\cos\alpha)/\sin\alpha, \tag{3}$$

$$=(W_t - D)(1-\cos\alpha)/\sin\alpha. \tag{4}$$

It follows from these equations, that for a given length of snake pivoted in a simple fashion, forward progression per cycle of movement is maximized when $\alpha = 90°$. Similarly, for any two snakes of equal diameter in tunnels of equal width, more forward movement per cycle is generated as α increases. For a given value of α, snakes with greater diameter will generate less forward movement per cycle because the effective tunnel width is less.

Table 2 lists observed mean values of α for an *Elaphe* (TL = 159 cm) and *Nerodia* (TL = 100 cm). Despite the fact that the *Elaphe* was longer than the *Nerodia*, the maximum diameter at midbody of *Nerodia* (3·4 cm) was greater than that of *Elaphe* (2·0 cm). Substituting observed values of α for a 7·5 cm tunnel and D values of these two snakes and solving for Δx_i, the predicted values of Δx_i of *Nerodia* and *Elaphe* are 2·6 and 4·5 cm, respectively. The total forward movement of the snake is simply the sum of the values calculated for the extension of each region between opposite sides of the tunnel. In 7·5 cm tunnels, these two snakes usually had five such regions, resulting in predicted values of overall forward movement per cycle for *Nerodia* and *Elaphe* of 13·0 and 22·7 cm, respectively. These predicted values agree fairly well with the respective observed mean values of 10·9 and 21·9 cm (Table 2). Hence, both the posture and the more elongate body form of *Elaphe* appear advantageous for concertina locomotion.

The ability of a snake to form a steep angle relative to the sides of the tunnel may be influenced by several factors. As seen in the comparison of *Elaphe* and *Nerodia*, more vertebrae of the *Elaphe* fit between opposite sides of the tunnel and no significantly greater maximal lateral vertebral flexion was required to obtain a value of α near 90°. In certain cases, the ability to obtain a steep angle between the body and the tunnel may be limited by the axial morphology of the snake. Either the nature of the vertebrae themselves or the relative diameter of the snake may limit the maximal lateral flexion of an animal.

Vertebral flexion

The potential effect of body diameter on vertebral flexion can be estimated with another simple model. In Fig. 16B three vertebrae are schematically represented by lines, each of length L_{vert}. Perpendicular to each vertebra is another line segment representing the distance from the midline to the lateral-most extent of a rib (= D/2). Assuming that physical contact of the ribs limits lateral flexion, one can solve for the maximal lateral vertebral flexion in terms of vertebral length (L_{vert}) and D/2. If the angle between the two adjacent touching ribs is β, then:

$$\tan(\beta/2) = (L_{vert}/2)/(D/2). \tag{5}$$

It can be shown that $\beta = \theta_{max}$. After substituting for $\beta = \theta_{max}$, solving for θ_{max} yields:

$$\theta_{max} = 2\tan^{-1}(L_{vert}/D). \tag{6}$$

For the *Nerodia* and *Elaphe* whose concertina locomotion was analysed above, values of L_{vert} at midbody were 0·62 and 0·63 cm, respectively. Predicted values of θ_{max} for these two snakes were 21° and 35°, respectively. Thus, even for the relatively stout *Nerodia* the width of the body is a poor predictor of maximal lateral vertebral flexion during locomotion (observed $\theta_{max} = 15°$). Equation 6 does predict a θ_{max} of less than 10° for values of D/L_{vert} greater than 12. Therefore, because D/L_{vert} exceeds 12 for some vipers within the genus *Bitis* (B. C. Jayne, personal observation), stout snakes such as these would be predicted to have extreme difficulty performing concertina locomotion because of the small effective tunnel width and a body width which could inhibit the relatively large amount of lateral vertebral flexion necessary for effective concertina locomotion.

Because the amount of vertebral flexion should affect the amount of stretch undergone by the contractile tissue within muscle segments, it is useful to examine maximal vertebral flexion among different locomotor modes and species. Jayne (1988) found that the maximal θ of *Nerodia* and *Elaphe* performing terrestrial lateral undulation seldom exceeded 5°. Maximal θ of swimming *Nerodia* is usually less than 5·5° and that of swimming *Elaphe* rarely surpasses 2° (Jayne, 1988). In this study, during sidewinding, both *Nerodia* and *Crotalus* had moderately high values of maximal θ of 7° and 10°, respectively. During the concertina locomotion of *Nerodia* and *Elaphe* maximal θ was less than or equal to 16°. Because of these differences in lateral flexion that occur even within a single species performing different locomotor modes, it seems likely that muscle architecture that maximizes performance for one locomotor mode may compromise performance in another locomotor mode (e.g. concertina *versus* lateral undulation). Similarly, Ruben (1977) suggested that optimal muscle morphology for constriction may compromise aspects of locomotor performance.

Patterns of segmentation

Much of the morphological diversity of snakes involves aspects of segmentation of the skeletal and muscular systems. The numbers of vertebrae in snakes range from about 160 to 400 (Hoffstetter & Gasc, 1969) and vertebral number is not simply correlated with interspecific differences in size (Johnson, 1955). The ratio of body vertebrae to caudal vertebrae and the length of the tail relative to the body also vary widely. The ratio of snake length to maximum diameter ranges from 15 for some vipers (Thomas & Pough, 1979) to more than 100 for some arboreal species (B. C. Jayne, personal observation), and this indicates tremendous differences in the stoutness of individual body segments.

Among different species, there is a variable relationship of muscle segments to body segments. The muscle fibres contributing to an individual epaxial muscle segment may arise from 2–6 adjacent body segments (Gasc, 1974; Jayne, 1982). The number of vertebrae spanned by axial muscles may vary either as a result of tendinous interconnections among muscles or from elongation of tendon within muscle segments. For example, the tendons of spinalis muscle segments may span from 3 to 37 vertebrae (Jayne, 1982).

A primary reason for studying both *Nerodia* and *Elaphe* is the great difference between their numbers of body vertebrae (125 *versus* 240). Despite these differences, the waveform and timing of muscle activity relative to vertebral flexion are similar for the swimming of these two taxa (Jayne, 1985*a*, 1988). Both *Nerodia* and *Elaphe* use similar portions of their bodies to form each undulation while they swim; however, *Elaphe* displays simultaneous activity in approximately twice the number of adjacent muscles compared with *Nerodia*. Hence, when similar proportions of the body are used in locomotion, increased recruitment of muscle segments in *Elaphe* appears to compensate for the increased number of body segments. During the concertina locomotion observed in this study, a similar trend emerged. For both *Nerodia* and *Elaphe*, as a greater number of body segments are necessary to span the opposite sides of the wider tunnels, increased numbers of adjacent muscle segments display simultaneous activity (Table 2). When tunnel widths are a similar proportion (6 %) of the total length of *Nerodia* and *Elaphe*, *Elaphe* often uses more than twice the number of vertebrae between opposites sides of the tunnel, and it compensates by having about twice as many simultaneously active adjacent muscle segments (Table 2, compare 5 and 7·5 cm tunnel widths).

The variable relative size and number of vertebrae of the tail suggest that the effectiveness of the tail as a propulsive organ varies considerably among snake taxa, but the consequences of caudal morphology probably vary with locomotor mode. The tail of *Nerodia* is about 25 % of its total length compared with 16 % for *Elaphe*; however, the swimming of these two taxa is very similar (Jayne, 1985*a*, 1988). For aquatic locomotion, the effect of relative tail length of the tapering tails found in most terrestrial snakes (e.g. *Nerodia* and *Elaphe*) is probably trivial compared with the effects of the distribution of surface area along the length (Graham *et al.* 1987). The results of this study suggest that the tail of snakes may not be effective for generating the movements and forces necessary for sidewinding (Fig. 14). Although the effects of different substrates cannot be totally discounted, it is very suggestive that *Crotalus*, which has a smaller relative tail length than *Nerodia* (8 % *vs* 25 % of total length), was able to establish areas of static contact with a much greater proportion of its entire length. Because the relative tail length varies from about 5 % to 33 % of total length among snake species (unpublished data from 94 species listed in Jayne, 1982), it would be of great interest to determine the importance of the tail for limbless locomotion.

The relationship of body width to vertebral length is one of the many ways in which the shape of individual body segments varies. This ratio of width to length affects concertina locomotion (Fig. 15; Table 2) and may constrain the vertebral flexion of some stout species (Fig. 16B). Relating mass per body segment to the shape and orientation of the ribs should be another productive area for future studies of the morphological diversity of the axial skeleton of limbless vertebrates.

To differing extents, the tendons that connect nonhomologous muscles intermingle with intermuscular septa. For example, in all three taxa of this study, a very distinct tendon extends between the M. longissimus dorsi and the medial head of the M. iliocostalis. Yet the variable nature of the septum between these two muscles made it difficult to determine if the origin of the M. iliocostalis is directly on a bone or if it attaches to a bone *via* the M. longissimus dorsi. Similarly, in *Nerodia* and *Elaphe*, the connection between the semispinalis and the M. longissimus dorsi is obscured by an intermuscular septum. Hence, the question arises as to what the functional origin and insertion may be for these interconnected muscle segments.

If simultaneous activity of a set of interconnected muscle segments occurs, then the set of contracting muscles might be considered to be a functional unit. Alternatively, if the interconnected segments of nonhomologous muscles are not active simultaneously, then the effective origins and insertions may be the bony element to which an attachment is most immediately made. For example, in *Nerodia* the contractile tissue of the LD is about eight vertebrae posterior to that of the connected SSP. Consequently, for combined function of the SSP and LD, the activity of the contractile tissue of the LD should be synchronous with an SSP segment eight vertebrae anterior to its location and should precede activity of an SSP with contractile tissue at the same level of the body. However, no consistent differences were observed in the onset or offset of activity that would support the combined function of either the SSP–LD (in *Nerodia* and *Elaphe*) or the LD–IC (in all three species). Instead, for the planar movements observed during lateral undulation (Jayne, 1988) and concertina locomotion (Fig. 10), there was usually synchronous activity of all the contractile tissue at a given region of the body. The ability to detect differential activity of adjacent nonhomologous muscles (Fig. 4) suggests that cross-talk (Loeb & Gans, 1986) was not responsible for these observations of synchronous activity. The LD of *Nerodia* and *Crotalus* showed similar timing of activity with respect to movement records (Figs 3 and 8) despite different connections of the medial tendon of this muscle. Furthermore, the different patterns of right- and left-side muscle activity observed for sidewinding (Figs 4 and 6), strongly suggest that there is no obligate joint function of interconnected muscles. Therefore, the anatomically interconnected epaxial muscles appear to be functioning independently.

The proportions of tendon and contractile tissue within a muscle segment may affect both force generation and the extent to which contractile tissue is stretched in convex regions of the body. These two factors could in turn affect the timing of muscle activity. Tendon length within muscle segments does vary among different muscles and taxa, and this variation has been of particular interest in studies of snake anatomy and locomotion (Mosauer, 1935; Auffenberg, 1961; Gasc, 1974; Ruben, 1977; Jayne, 1982). Dividing the length of contractile tissue by the total length of a muscle segment indicates the extent of tendinous elongation. For *Nerodia*, *Elaphe* and *Crotalus*, the respective percentages of contractile tissue per muscle segment are about 25 %, 28 % and 32 % for the SSP-SP, 67 %, 67 % and 62 % for the LD and 67 %, 67 % and 84 % for the IC. Thus the proportion of contractile tissue generally increases from more medial to more lateral muscles within each species. A closer examination of the activity of the IC during the sidewinding of *Nerodia* and *Crotalus* reveals that major activity of the IC often did not begin until a region was almost straight and continued until the region was maximally flexed. This time of major activity, combined with the lateral location of this muscle and its relatively high proportion of contractile tissue, suggests there may indeed be different optimal times for the various muscles to affect lateral flexion. However, a quantitative approach beyond the scope of this study will be necessary to resolve this issue.

Comparison of locomotor modes

Lateral undulation, sidewinding and concertina are the three primary modes of terrestrial snake locomotion that use vertebral flexion to generate propulsive forces (Gray & Lissmann, 1950; Gans, 1974; Edwards, 1985). For all these modes, the Mm. semispinalis-spinalis and multifidus were implicated as dorsiflexors in addition to the correlation of their activity with lateral vertebral flexion observed for planar movements. The remaining muscles studied, including the Mm. longissimus dorsi and iliocostalis, all appear to function as lateral vertebral flexors. Furthermore, large numbers of adjacent segments of these muscles usually show synchronous activity during locomotion.

Opinions differ about the relationship of sidewinding to other modes. Gray (1946) and Brain (1960) suggested that sidewinding was derived from lateral undulation because of the continuous propagation of a wave of lateral flexion in both these modes. As discussed by Jayne (1986), the existence of a transitional mode combining lateral undulation and sidewinding could support the idea that sidewinding was derived from lateral undulation. Jayne (1988) illustrated a sequence of terrestrial lateral undulation of *N. fasciata* during which there was slight bilateral activity of the SP. Hence, bilateral activity can apparently be superimposed on a pattern of muscle activity characteristic of terrestrial lateral undulation, and the extent of bilateral activity of the dorsiflexors will determine whether sidewinding occurs. Muscle activity in sidewinding and lateral undulation ceases when a region becomes maximally concave, whereas concertina locomotion often has prolonged concave-side activity. This evidence further suggests a close relationship of sidewinding to terrestrial lateral undulation.

Although Gans (1974) did not unequivocally state that sidewinding was derived from concertina locomotion, he stressed the commonality of static contact in these two modes. The profiles of linear velocities (V_r) used in this study tend to emphasize the momentary static contact with the substrate seen in both sidewinding and concertina locomotion, agreeing with Gans' (1974) analysis. However, the profiles of $\bar{\theta}$ often revealed continuous transitions of the snake from convexity to concavity during sidewinding (Figs 3, 7 and 8). As snakes contacted the substrate during sidewinding, the linear velocities would equal zero, but angular velocities (slope of $\bar{\theta}$ *versus* time) of the vertebral column changed continuously. Continuous change in angular velocities indicates the continuous propagation of a wave of lateral bending, and this supports the suggestion of Gray (1946) and Brain (1960) linking sidewinding with lateral undulation.

A striking unifying feature of axial muscle activity during terrestrial snake locomotion (Jayne, 1988 and this study) is the lack of lateral flexor activity while the contractile tissue is being elongated (as indicated by vertebral flexion). In contrast, there is activity during the elongation of lateral flexors in the posterior region of swimming snakes (Jayne, 1988). Recent studies of the terrestrial locomotion of reptiles (Jenkins & Goslow, 1983) and mammals (Goslow *et al.* 1981) have also documented significant (eccentric) activity of limb muscles while they lengthen. If the relationship of activity to the stretching of muscle were similar among different species of snakes performing the same locomotor mode, then changes in segmentation and axial morphology might be tightly integrated; future comparative studies would be very useful for resolving this issue. Furthermore, the observed lack of eccentric muscle activity in snakes during terrestrial locomotion may point to one more of the many interesting fundamental differences between limbless and limbed locomotion.

This work is based on part of a PhD dissertation submitted to the Department of Zoology at Michigan State University. Financial support was provided by National Science Foundation Dissertation Improvement grant no. BSR-8401874 and grants from the Michigan State University and National Chapters of Sigma Xi, The Research Society, as well as from NIH grant NS16270 to J. Edwards. J. Edwards, my advisor, provided much encouragement and support throughout my dissertation work, and he, G. Lauder and P. Wainwright offered helpful criticisms of an earlier draft of this manuscript. D. Straney and J. Vorro provided necessary facilities and equipment. P. Ocello, C. D'Haem, C. Cheng, K. McWilliams, S. DosReis, J. Zablotny, C. Griffith and C. Jayne helped with animal care and filming. J. Zablotny prepared the muscle illustration.

References

AUFFENBERG, W. (1961). Additional remarks on the evolution of trunk musculature in snakes. *Am. Midl. Nat.* **105**, 241–291.

BRAIN, C. K. (1960). Observations on the locomotion of the Southwest African adder, *Bitis peringueyi* (Boulenger), with speculations on the origin of sidewinding. *Ann. Transvaal Mus.* **24**, 19–24.

Edwards, J. L. (1985). Terrestrial locomotion without appendages. In *Functional Vertebrate Morphology* (ed. M. Hildebrand, D. M. Bramble, K. F. Liem & D. B. Wake), pp. 159–172. Cambridge: Belknap Press of Harvard University Press.

Fetcho, J. R. (1986). The organization of the motoneurons innervating the axial musculature of vertebrates. II. Florida water snakes (*Nerodia fasciata pictiventris*). *J. comp. Neurol.* **249**, 551-563.

Fetcho, J. R. (1987). A review of the organization and evolution of motoneurons innervating the axial musculature of vertebrates. *Brain Res. Rev.* **12**, 243–280.

Gans, C. (1974). *Biomechanics. An Approach to Vertebrate Biology.* Ann Arbor: University of Michigan Press.

Gans, C. (1985). Limbless locomotion – a current overview. In *Proceedings of the International Symposium on Vertebrate Morphology,* pp.13–22. Stuttgart, New York: Gustav Fischer Verlag.

Gans, C. & Mendelssohn, H. (1972). Sidewinding and jumping progression of vipers. In *Toxins of Animal and Plant Origin,* vol. 1 (ed. A. de Vries & E. Kochva), pp. 17–38. London: Gordon & Breach.

Gasc, J. P. (1967). Introduction a l'étude de la musculature axiale des squamates serpentiformes. *Mém. Mus. natn. Hist. nat., Paris (Zool.)* **48**, 69–124.

Gasc, J. P. (1974). L'interpretation fonctionelle de l'appareil musculosquelettique de l'axe vertebral chez serpents (Reptilia). *Mem. Mus. natn. Hist. nat., Paris (Zool.)* **83**, 1–182.

Gasc, J. P. (1981). Axial musculature. In *Biology of the Reptilia,* vol. 11 (ed. C. Gans & T. S. Parsons), pp. 355–435. New York: Academic Press.

Goslow, G. E., Jr, Sheerman, H. J., Taylor, C. R., McCutchin, M. N. & Heglund, N. C. (1981). Electrical activity and relative length changes of dog limb muscles as a function of speed and gait. *J. exp. Biol.* **94**, 15–42.

Graham, J. B., Lowell, W. R., Rubinoff, I. & Motta, J. (1987). Surface and subsurface swimming of the sea snake *Pelamis platurus. J. exp. Biol.* **127**, 27–44.

Gray, J. (1946). The mechanism of locomotion in snakes. *J. exp. Biol.* **23**, 101–120.

Gray, J. (1953). Undulatory propulsion. *Q. J. microsc. Sci.* **94**, 551–578.

Gray, J. (1968). *Animal Locomotion.* London: Weidenfield & Nicholson.

Gray, J. & Lissmann, H. W. (1950). The kinetics of locomotion of the grass snake. *J. exp. Biol.* **26**, 354-367.

Hoffstetter, R. & Gasc, J. P. (1969). Vertebrae and ribs of modern reptiles. In *Biology of the Reptilia* (ed. C. Gans & T. S. Parsons), pp. 201-302. New York: Academic Press.

Jayne, B. C. (1982). Comparative morphology of the semispinalis-spinalis muscle of snakes and correlations with locomotion and constriction. *J. Morph.* **172**, 83–96.

Jayne, B. C. (1985*a*). Swimming in constricting (*Elaphe g. guttata*) and nonconstricting (*Nerodia fasciata pictiventris*) colubrid snakes. *Copeia* **1985**, 195–208.

Jayne, B. C. (1985*b*). Mechanisms of snake locomotion: an electromyographic study. PhD thesis. Michigan State University.

Jayne, B. C. (1986). Kinematics of terrestrial snake locomotion. *Copeia* **1986**, 915–927.

Jayne, B. C. (1988). Muscular mechanisms of snake locomotion: An electromyographic study of lateral undulation of the Florida banded water snake (*Nerodia fasciata*) and the yellow rat snake (*Elaphe obsoleta*). *J. Morph.* (in press).

Jenkins, F. A., Jr & Goslow, G. E., Jr (1983). The functional anatomy of the shoulder of the savannah monitor lizard (*Varanus exanthematicus*). *J. Morph.* **175**, 195–216.

Johnson, R. G. (1955). The adaptive and phylogenetic significance of vertebral form in snakes. *Evolution* **9**, 267–288.

Loeb, G. E. & Gans, C. (1986). *Electromyography for Experimentalists.* Chicago: University of Chicago Press.

Mosauer, W. (1932). On the locomotion of snakes. *Science* **76**, 583–585.

Mosauer, W. (1935). The myology of the trunk region of snakes and its significance for ophidian taxonomy and phylogeny. *Publs Univ. Cal. Los Angeles biol. Sci.* **1**, 81–121.

Ruben, J. A. (1977). Morphological correlates of predatory modes in the coachwhip (*Masticophis flagellum*) and rosy boa (*Lichanura roseofusca*). *Herpetologica* **33**, 1–6.

Thomas, R. G. & Pough, F. H. (1979). The effect of rattlesnake venom on digestion of prey. *Toxicon* **17**, 221–228.